Feasibility of Extractive Distillation in a Batch Rectifier

Z. Lelkes and P. Lang
Dept. of Chemical Engineering, Technical University of Budapest, H-1521 Budapest, Hungary

B. Benadda and P. Moszkowicz
INSA de Lyon, LAEPSI, 69621 Villeurbanne, France

A simple method was developed to study the feasibility of extractive distillation in a batch rectifier. By calculating feasible profiles of different column sections and figuring them in the triangular diagram, the feasibility and limiting values of the most important operational parameters (number of stages, flow rate of entrainer, and reflux ratio) were determined for different steps of the batch extractive distillation. The unusual behavior of extractive distillation was also investigated for this process. An infeasible region can be assigned to the given values of parameters; if the still composition is located within this region, the specified separation cannot be attained. By locating this infeasible region, maximum recoveries attainable in a batch rectifier and in a middle vessel column were compared. The results obtained by this method were verified by pilot-plant experiments for the mixture acetone-methanol + water.

Introduction

Batch distillation is a classical and very important separation method in the chemical industries. It is applied, among others, to pharmaceutical and speciality chemical manufacturing to recover the components from waste-solvent mixtures. These mixtures frequently form azeotropes that cannot be separated by conventional rectification; that is why for this purpose a special distillation method must be applied. One of the most important special methods is the extractive (homoazeotropic) distillation. The continuous extractive distillation is a well-known, widespread technology in the chemical industries. However, the batch extractive distillation (BED) is not used in the industry enough although it can simultaneously provide the advantages of both batch and extractive distillations. When a chemical process is designed, the most important issue is always feasibility; thus, it is necessary to assess process feasibility before making the design specifications. Feasibility studies also contribute to the better understanding of complex unit operations such as the batch extractive distillation.

Bernot et al. (1990, 1991) studied the patterns of composition change, feasibility and separation sequencing in multicomponent batch distillation. In their article, the general behavior of ternary azeotropic distillation was described in simple terms based on the nature of the distillate and still composition changes in the phase plane. Using residue curve maps, they identified the boundaries and distillation regions for the batch separation of azeotropic mixtures. They developed a systematic procedure for assessing the feasibility of multicomponent azeotropic mixtures in batch rectifiers and strippers. Using only residue curve maps, the product sequences for these mixtures were identified at infinite reflux (reboil) ratio and at infinite number of stages. They also described methods of breaking azeotropes by using a homogeneous entrainer. However, they did not investigate the effect of continuous feeding of the entrainer. The theory of using residue curve maps for the analysis of batch distillation of homogeneous mixtures was generalized and extended to systems with an arbitrary number of components by Ahmad and Barton (1996).

Safrit et al. (1995, 1997) extended the method of Wahnschafft et al. (1992, 1993), suggested for the assessment of the feasibility of the continuous conventional and extractive distillation, to batch distillation. They pointed out that in the case of batch distillation the still and product compositions change with time, so the basic feasibility analysis covers only an instant in time. According to these authors, the determi-

Correspondence concerning this article should be addressed to P. Lang, who is currently at the Dept. of Chemical and Food Engineering.

nation of the instantaneous profiles and the regions of the instantaneous feasible products can be carried out by the application of the method used for continuous distillation. The regions of possible column profiles can be identified for the specified product compositions. These are bounded by the total reflux curve (approximated by the residue curve passing through the product composition) and the product pinch point curve. According to this method, the triangular diagram can be divided into feasible and infeasible regions for extractive distillation. For the determination of these regions, the graphical method of Wahnschafft et al. (1993) developed for continuous extractive distillation was suggested. For the assessment of the feasibility of the extractive distillation, they considered the operation of the extractive section of the column. For performing the BED, they suggested the use of a middle vessel column that makes possible the simultaneous regeneration of the entrainer during the production.

In our earlier articles a basic (R = const.) operational policy for performing the BED in batch rectifiers was presented and analyzed by pilot-plant experiments and simulation (Yatim et al., 1993; Lang et al., 1994). The importance of the continuous entrainer feeding and of its molar volume was also demonstrated. In the second phase of the work (Lang et al., 1995; Lelkes et al., 1997), the basic operational policy was improved and several further operational policies (e.g., $x_{D,A}$ = const.) were studied experimentally and by simulation. By using optimization criteria and introducing an objective function, these policies were compared. So far the proper feasibility analysis of the BED process has not been made, though this could provide useful information [e.g., N_{min}, R_{min}, $(F/V)_{min}$] when designing BED separations. The goal of this article is to present a method for assessing the feasibility of this process.

Feasibility Methods for Multicomponent Batch Distillation

Batch distillation of ternary mixtures

In the case of sufficiently large reflux ratio (R) and number of theoretical stages (N) the liquid composition profiles in the column follow the simple distillation residue curves, so the instantaneous distillate (x_D) and still compositions (x_s) are on the same residue curve (Bernot et al., 1990). Each still path follows a straight line determined by the initial still (charge) composition (x_{ch}) and the distillate composition (unstable node) until it reaches either the edge of the triangle or a simple distillation stable separatrix (Figure 1). Then, the path follows these limiting curves up to a stable node. On the basis of these facts, the triangle can be divided into batch distillation regions for any ternary mixture. In a given region, the number of fractions and their sequence are characteristic of this area. This method is shown in Figure 1 and Table 1 where the distillation regions of a ternary mixture having a residue curve map characteristic of the extractive distillation are seen. [The binary mixture A-B forms a minimum boiling point azeotrope; the third component (E) is the heavy entrainer. The ternary mixture has a residue curve map 100 by the classification of Matsuyama and Nishimura (1977) and Doherty and Perkins (1979).]

It can be concluded from the results of Table 1 that the extractive distillation cannot be efficiently performed in batch if the entrainer is added to the charge at once before the beginning of the distillation, since the azeotrope cannot be broken in this way.

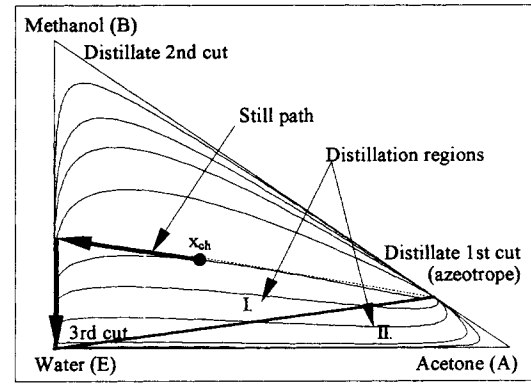

Figure 1. Still path and distillation regions for a mixture with residue curve map 100 in the case of high number of stages and reflux ratio.

Feasibility of batch extractive distillation by Safrit et al. (1995)

To assess the feasibility of batch extractive distillation, Safrit et al. (1995) proposed the graphical method of Wahnschafft et al. (1992, 1993) developed for continuous extractive distillation. In batch distillation the still and product compositions change with time and thus the basic feasibility analysis only covers an instant in time. They also described that the still composition is also a tray composition, therefore, it must lie on the column profiles just like any other tray compositions. To assess the feasibility of extractive distillation, they investigated the operation of the extractive section of the column.

By writing the mass balances for this section (Figure 2) for the given distillate flow rate (D), entrainer molar flow rate (F), and molar compositions (x_D, z), a Δ point can be determined where all operating (mass balance) lines intersect:

$$V_{j+1} + F = L_j + D \tag{1}$$

$$V_{j+1} - L_j = F - D = \Delta \tag{2}$$

$$x_{\Delta,i} = \frac{D \cdot x_{D,i} - F \cdot z_i}{D - F} \quad i = 1, \ldots, 3 \tag{3}$$

Above authors drew tangents to the residue curves from the point Δ. The curves formed by these tangent points were

Table 1. Sequence of Fractions for a Mixture with a Residue Curve Map 100

Distillation	No. of Fractions	Sequences
I	3	1st cut: A-B azeotrope 2nd cut: B 3rd cut: E
II	3	1st cut: A-B azeotrope 2nd cut: A 3rd cut: E

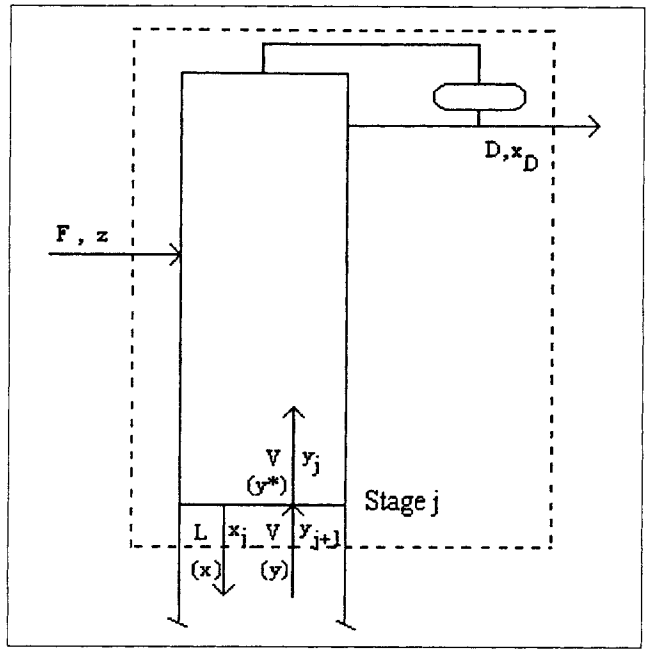

Figure 2. Scheme for writing mass balances for the extractive section.

named Δ pinch point curves. They stated that each point of these curves is a pinch (fixed, stationary) point and the Δ pinch point curves with the edges of the triangular diagram limit regions, in which the extractive section does not work as required. As a result, the column cannot produce the intended (specified) distillate product (Figure 3).

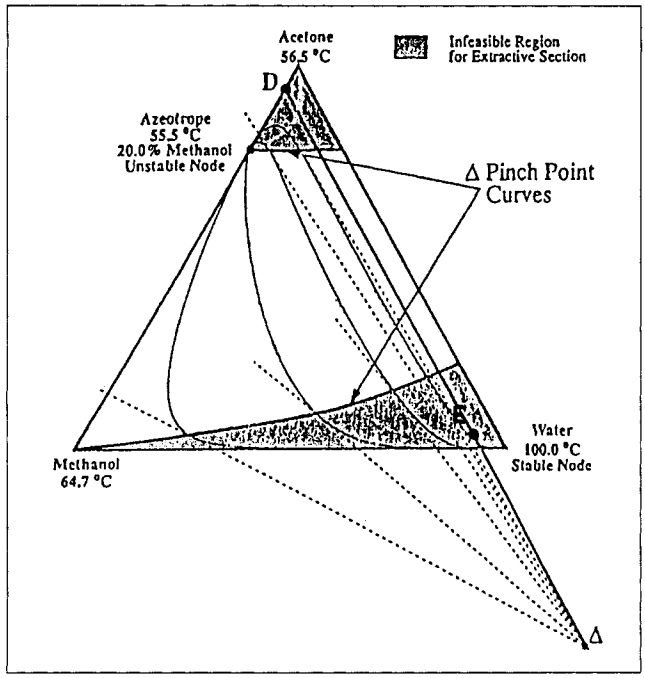

Figure 3. Feasible and infeasible regions by the method of Safrit et al. (1995).

Safrit et al. (1995) state that if the still composition is in the infeasible region, the extractive section is not able to maintain the separation acetone/methanol and methanol appears in the distillate. On the basis of Figure 3 from a mixture with fixed acetone content (e.g., $x_A = 0.1$), a given composition distillate product can be obtained by extractive distillation (with the given entrainer flow rate and composition) if the methanol concentration (x_B) is high [to the detriment of water content (x_E)]. However, this product quality cannot be reached if the methanol concentration is low. This conclusion was in contradiction with the result of our experiments and calculations; therefore, we have investigated whether the regions in the figure are really infeasible regions or not.

Pilot-plant experiment of batch extractive distillation

We compared the results that were obtained by the feasibility method of Safrit et al. (1995) with the results of our experiments and calculations for the basic operational policy (R = const., F = const.). The most important data of the column are: 32 bubble cap plates, the feed is introduced to stage 7 (stages are numbered from the top), diameter = 0.1 m, reboiler volume = 12 dm^3, holdup ≅ 40 cm^3/plate.

For the rigorous simulation of the pilot-plant experiment, the following input data were used. The charge to be separated contains 50-50 mol % A and B, respectively. Its volume is 9 dm^3. The heat duty of reboiler $Q_{N+1} = 1.5$ kW, $P = 1.013$ bar, the reflux is boiling point liquid, $R = 4$. The temperature of the entrainer (pure water) is 70°C, $F = 2$ dm^3/h. The model has 18 theoretical stages, and the feed stage is the 6th. [The volumetric holdup (H_j^{vol}) assumed for a theoretical stage is then 71 cm^3, its value for the condenser is 100 cm^3.] The specified product purity is: $x_{D,A} = 94\%$, $x_{D,M} = 2.5\%$, $x_{D,W} = 3.5\%$. For describing vapor-liquid equilibrium conditions, the UNIQUAC model was used with the data published by Griswold and Buford (1949). The simulation of the pilot-plant experiment was performed by the Distefano (1968) method (Yatim et al., 1993).

At first, the Δ pinch point curves were determined by the Safrit et al. (1995) method for our data (Lang et al., 1995). We have found that for the given distillate product composition and flow rate with the given entrainer flow rate and composition on a Δ pinch point curve, maximum two real pinch points are located. In the case of a real pinch point the equilibrium composition of vapor (y^*) leaving the tray (having liquid composition x) is the same as that of vapor (y) arriving at this tray satisfying the material balances for the extractive section (Figure 2). For the points of the two curves obtained by graphical method (Δ 'pinch point' curves), we determined the equilibrium compositions (y^*) and from the material balances the vapor compositions (y) (see Figure 4). It can be stated that the y^*-curve and the y-curve intersect only at two points on the lefthand side 'pinch point' curve and that on the righthand side 'pinch point' curve the y^*-curve and the y-curve do not meet at all. It must be concluded that *if the line through Δ and x is a tangent to the residue curve passing through x, this condition is necessary but not sufficient for x being a fixed (pinch) point*, because this does not necessarily imply the equality of equilibrium and arriving vapor compositions.

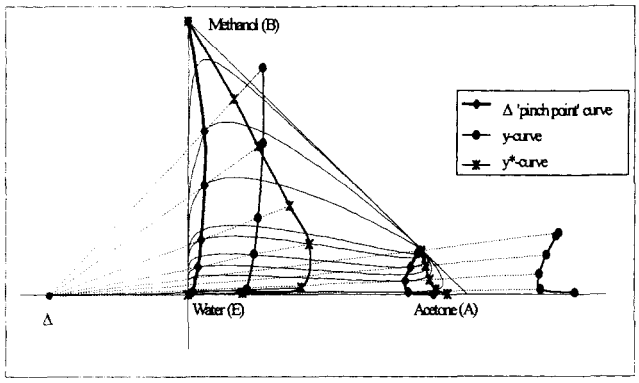

Figure 4. Δ 'pinch point,' y^*- and y-curves for the BED.

$D = 0.0096$ mol/s; $x_D = [0.94, 0.025, 0.035]$; $F = 0.0278$ mol/s; $z = [0.0, 0.0, 1.0]$.

In Figure 5 a column profile calculated for the above example is also presented. Although the still composition is already within the 'infeasible' region, the extractive section is still working well, and methanol has not appeared in the distillate yet. The evolution of measured and simulated distillate compositions for the above experiment is shown in Figure 6. The still composition ($x_s = [0.023, 0.229, 0.748]$) reached the Δ 'pinch point' curve at $t = 150$ min. In spite of this the distillate purity did not decrease significantly for about 20 minutes.

Taking these facts into consideration, we can conclude that the above feasibility method must be revised.

Calculation of Column Profiles for the Batch Extractive Distillation

Basic steps of the BED

A complete BED process consists of the following basic steps (Yatim et al., 1993):

1. Operation under total reflux without entrainer feeding.
2. Operation under infinite reflux ratio with entrainer feeding (purification of the distillate).
3. Operation under finite reflux ratio with entrainer feeding (production of A).

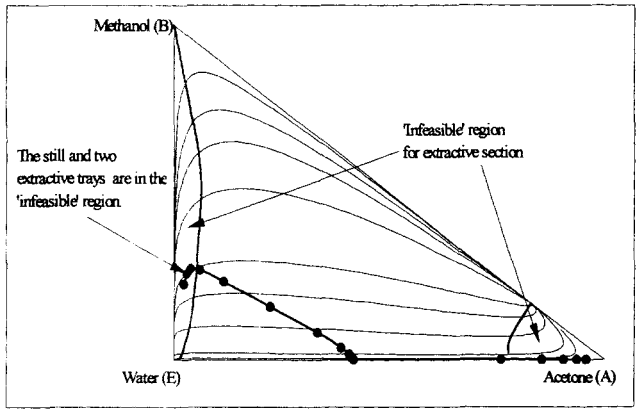

Figure 5. Column profile for a pilot-plant experiment.

$t = 160$ min; $\Delta t_2 = 60$ min. The extractive profile penetrates into the 'infeasible' region.

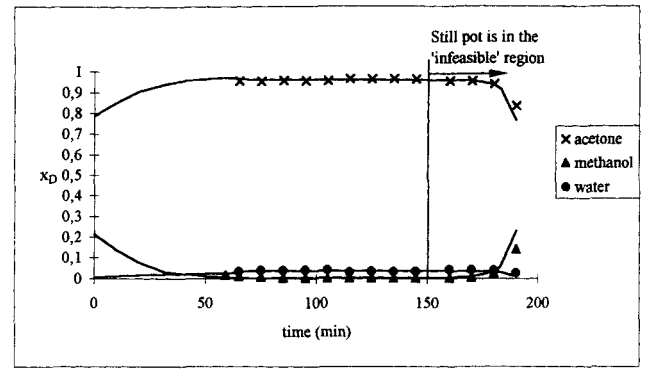

Figure 6. Evolution of the distillate composition for a pilot-plant experiment.

4. Operation under finite reflux ratio without entrainer feeding (separation of the component B from the entrainer).

Model

The BED is performed under continuous entrainer feeding in a batch rectifier (Figure 7), containing a total condenser producing liquid at its boiling point, N stages in the column, [stages are numbered from the top, feed (saturated liquid) arrives at stage f] and a still (stage $N+1$). For preliminary design and synthesis, when we determine the basic pattern of the variation in the still, the tray and the distillate compositions with time, it is sufficient to apply a simplified model (Doherty and Caldarola, 1985). The following simplifying assumptions (see Bernot et al., 1990) were applied:

- Theoretical stages (except for the condenser)
- Negligible holdup (except for the still)
- Constant molar overflow (CMO)
- Quasi-steady state in the column.

Stages above the feed stage form the solvent recovery section named rectifying section (RS). The feed stage and the stages below it (including the still) provide the extractive section (ES) of the column.

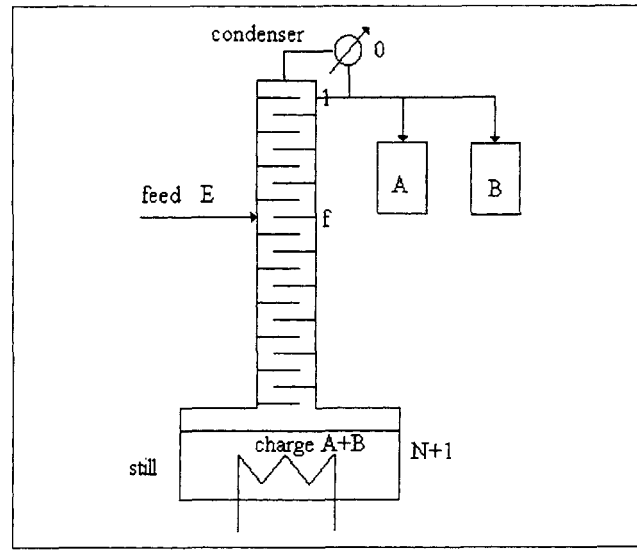

Figure 7. Batch extractive distillation column.

Calculation of the concentration profiles

To determine the possible instantaneous concentration profiles of the two sections, an approximate differential model was applied (see among others Van Dongèn et al.,1985; Fidkowski et al., 1991, 1993) since it makes possible the radical reduction of the size of the problem and allows direct comparison with the simple distillation residue curves.

When a possible profile is calculated, the value of the following parameters will be specified: entrainer and distillate flow rates and compositions, heat duty in the still (Q_{N+1}) determining the vapor flow rate of the column (V). The scheme of a stage in the interior of any section of the column is shown in Figure 8.

For this stage the following material balances can be written:

$$L(x_j - x_{j-1}) = V(y_{j+1} - y_j) \tag{4}$$

With Eq. 4, the liquid composition of the next higher stage $(j-1)$ can be expressed in the following way:

$$x_{j-1} = \frac{V}{L}(y_j - y_{j+1}) + x_j \tag{5}$$

Taking into consideration that y_j is in equilibrium with x_j ($y_j = y^*$) and y_{j+1} can be calculated as a function of x_j from the material balances (Figure 2) written around stage j and the condenser ($y_{j+1} = y$), x_{j-1} can be computed from x_j by

$$x_{j-1} = \frac{V}{L}(y^* - y) + x_j \tag{6}$$

We can also express the liquid composition x_{j-1} by expanding it as a Taylor series about the liquid composition x_j, neglecting the terms higher than first order

$$x_{j-1,i} = x_{j,i} + \left.\frac{dx_i}{dh}\right|_{h=j} \cdot \Delta h \tag{7}$$

where $\Delta h = (j-1) - j = -1$.

Combining Eqs. 6 and 7 allows us to write

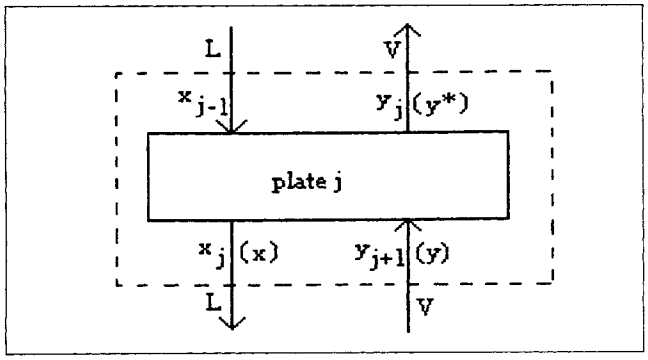

Figure 8. Inner stage of the rectifying or extractive section.

$$\frac{dx_i}{dh} = \frac{V}{L} \cdot (y_i - y_i^*). \tag{8}$$

By this general formula, the profiles for both sections can be easily determined. Equation 8 clearly shows the driving force of the mass transfer, namely, the difference between the composition of the vapor flow and the composition in equilibrium with that of the countercurrent liquid ($y - y^*$). By this differential equation for any initial liquid composition in the triangle, we can compute the profile where this composition can be located.

In Eq. 8 the value of V/L and the function $y(x)$ can be calculated for the different sections by the following formulas

Rectifying section:

$$\frac{V}{L} = \frac{V}{V - D} \tag{9}$$

$$y_i = \frac{(V - D) \cdot x_i + D \cdot x_{D,i}}{V} \tag{10}$$

Extractive section:

$$\frac{V}{L} = \frac{V}{V + F - D} \tag{11}$$

$$y_i = \frac{(V + F - D) \cdot x_i - F \cdot z_i + D \cdot x_{D,i}}{V} \tag{12}$$

In the case of total reflux for the rectifying section $V/L = 1$ and $y = x$, and differential Eq. 8 gives

$$\frac{dx_i}{dh} = (x_i - y_i^*) \tag{13}$$

This equation has a form identical with the simple distillation residue curve equation. Hence, in the rectifying section, near the total reflux the composition profiles will practically coincide with some portion of a simple distillation residue curve passing through this initial point.

Feasibility of the BED Process

In this section the four basic steps of the BED will be investigated from the point of view of feasibility. We shall consider the separation of a minimum boiling point azeotropic mixture using a heavy entrainer (acetone-methanol + water as entrainer) which is the most common application of the homogeneous azeotropic distillation. The method to be presented can be easily extended to the extractive distillation of other types of mixtures (maximum boiling azeotropes and mixtures with low relative volatility).

Feasibility means that for a mixture (charge) of a given composition (x_{ch}) a product (distillate) of specified composition can be reached by BED with the entrainer of a given composition. The separation will be considered feasible if there is an instantaneous state of the column, which provides the required quality product, starting the operation from the charge of the given composition. This means that the separation is feasible by BED if at least one point of the still path

and one point of the rectifying section profile starting from the specified product can be connected by an extractive profile.

Step 1 has no significance from the point of view of feasibility, it only serves for the heating up of the column. In our case, at the end of this step the azeotropic composition can be reached at the top.

Feasibility for Step 2

Step 2 is of key importance from the standpoint of feasibility, because the product is purified in this step from the azeotropic composition (breaking of the azeotrope) by continuous entrainer feeding under infinite reflux ratio. Achieving the required distillate purity in Step 2 means that the separation is feasible.

In Step 2 the still path depends only on the composition of the charge and that of the entrainer feeding since there is no distillate withdrawal. The variation of the still composition with time can be calculated from the material balances:

$$\frac{d(H_S \cdot x_S)}{dt} = + F \cdot z \qquad (14)$$

where the initial condition $x_S(0) = x_{ch}$.

The possible still compositions lie on the line connecting the charge and entrainer compositions. The starting point is the composition of charge, and then the still composition moves toward the entrainer composition, which could be achieved after infinite time. Since the reflux ratio is infinite, the only possible profile in the rectifying section lies between the distillate and entrainer vertex on the residue curve passing through the required distillate composition (Figure 9). In the majority of the cases this profile runs near the edge of the triangle.

The necessary and sufficient condition of the feasibility is to have at least one extractive section profile which connects the still path with the rectifying profile. For the given F/V ratio we can determine the possible extractive profiles starting from any still compositions by Eq. 8. This method is presented in Figure 10 for the data of the above experiment. The possible extractive profiles cross the rectifying profile, therefore, the separation is feasible. After meeting the rectifying profiles, the extractive profiles, arrive at the extraction section stable node (SN) located on the AE edge.

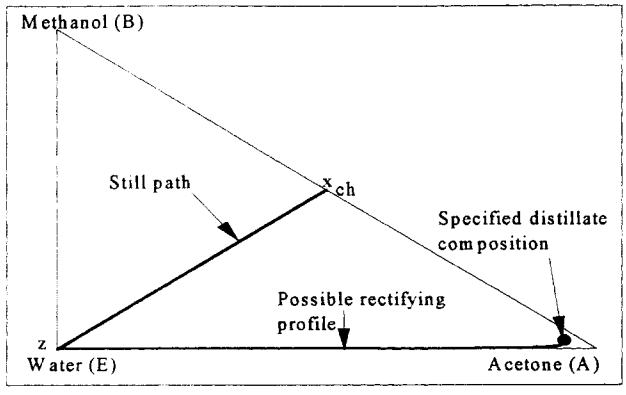

Figure 9. Still path and the rectifying profile in Step 2.

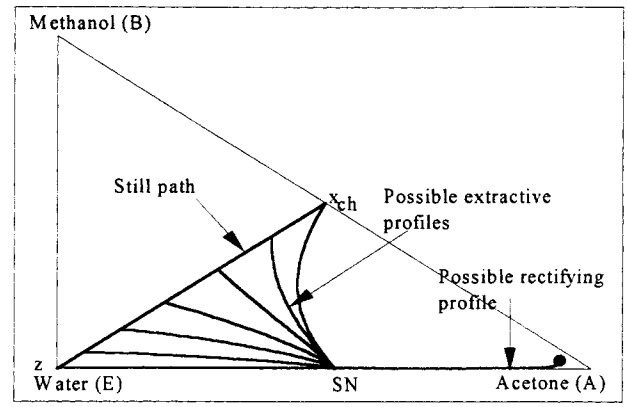

Figure 10. Extractive profiles starting from the still path in Step 2 for a feasible separation.

$F = 0.0278$ mol/s, $V = 0.048$ mol/s.

More information can be obtained if, similar to the residue curve map, we draw the possible extractive profiles in the whole area of the triangle for the given F/V ratio. Figure 11 shows the residue curve map and the map of possible extractive profiles for the above example and a profile calculated for the end of Step 2 ($R = \infty$, $F > 0$). We can state that under this F/V ratio from each point of the triangle the profiles arrive at the AE edge, therefore in that case there is no infeasible region. [However, by the graphical method of Safrit et al. (1995), the isovolatility curve ($\alpha_{A,B} = 1$) was obtained as a boundary.]

Figure 11 also shows that the extractive section has two fixed points (for continuous extractive distillation, see Knapp et al., 1994): a saddle-point (S_2) and a stable node (SN). S_2 originates from vertex B whereas SN comes from the azeotropic point which means that in the limiting case $R = \infty$, $F = 0$ these fixed points are located in vertex B and in the azeotropic point, respectively. On increasing the entrainer flow rate, both fixed points move toward vertex E. Between these fixed points there is a separatrix. This separatrix crosses the boundary of the conventional batch rectification (starting

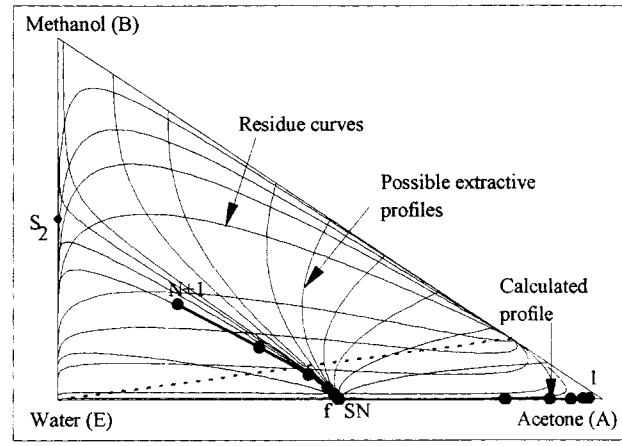

Figure 11. Column profile at the end of Step 2 on the map of the residue curves and extractive profiles.

$t_2 = 78$ min.

from the azeotropic point, dashed line), which separates the two distillation regions and the separatrix reaches the AE edge. In this way, the extractive profiles can also cross this boundary and can arrive at the AE edge, and in the rectifying section only components A and E must be separated. Hence, separations that cannot be performed by conventional batch rectification can be accomplished by BED. The computed profiles of the two sections show acceptable agreement with the possible ones; the profile from the still pot up to the entrainer feed stage follows an extractive profile and in the rectifying section tray compositions lie on the residue curve.

The map of the extractive profiles also indicates the component that can be obtained in Step 3 as a product. This depends on the location of the extractive section stable node. If it lies on the AE edge (or behind it) component A, if it is on the BE edge (or behind it) component B can be obtained as top product in Step 3.

One of the most important operational parameters of the BED is the flow rate of the entrainer under the given heat duty in the still. In the case of CMO, the constancy of Q_{N+1} results in a constant vapor flow rate. If the separation is feasible with a particular entrainer flow rate, there must be a *minimum flow rate*, since the separation is infeasible under $F = 0$ as shown in Figure 1. The value of the minimum flow rate depends on the vapor flow rate and the distillate flow rate that depends on the reflux ratio besides the compositions of the feed and distillate. If the flow rate of the entrainer feeding is below the minimum, then the extractive section stable node does not lie on or outside the AE edge but in the interior of the triangle. If SN is located within the triangle, all possible extractive profiles run into this point, so the extractive profile cannot reach the AE edge, that is, it cannot meet an appropriate rectifying profile which would provide high enough acetone purity. Figure 12 shows two maps of extractive profiles: in the first case (a) the entrainer flow rate is higher, whereas in the second (b) it is lower than the minimum.

To determine the location of SN and the value of the minimum entrainer flow rate, the bifurcation theory approach (Fidkowski et al., 1991,1993; Knapp and Doherty, 1994) for continuous extractive distillation could be extended for the BED. However, for Step 2 if the entrainer is pure, as it is common, the following simple methods can also be applied. As it has already been discussed, the necessary condition for a point to be a fixed one is that the line through Δ and $\boldsymbol{x}$ be a tangent to the residue curve passing through composition $\boldsymbol{x}$. In our case, $R = \infty$ ($D = 0$), $z = [0,0,1]$ (pure entrainer), therefore Δ coincides with the entrainer vertex. If $\boldsymbol{x}$ is a potential fixed point, then Δ, $\boldsymbol{x}$, $\boldsymbol{y}$ and $\boldsymbol{y}^*$ lie on the same line. Expressing the slope of this straight line in three different ways yields

$$\frac{x_B - 0}{x_A - 0} = \frac{y_B - 0}{y_A - 0} = \frac{y_B^* - 0}{y_A^* - 0} \tag{15}$$

From this equation we get

$$\frac{y_B^*}{x_B} = \frac{y_A^*}{x_A} \tag{16}$$

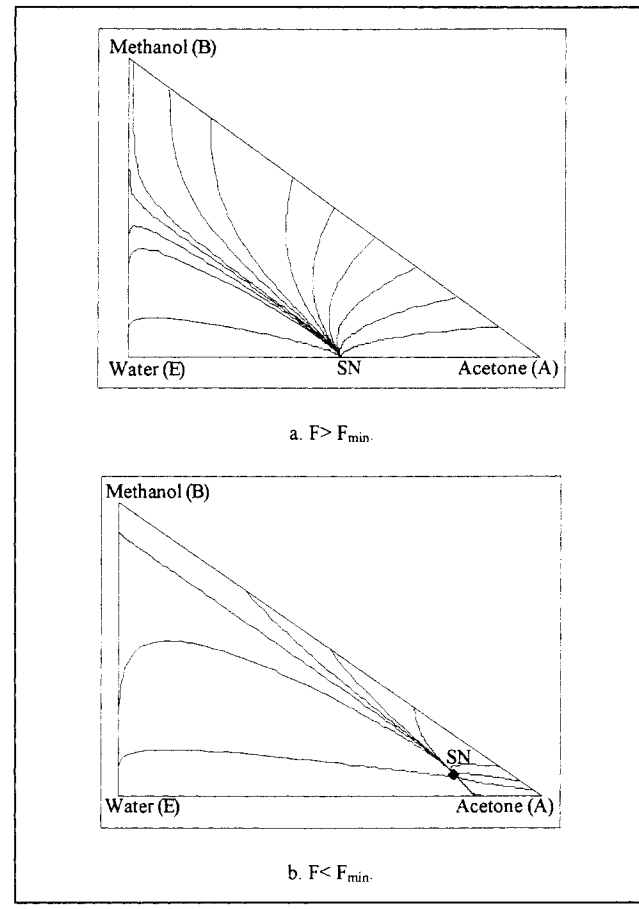

Figure 12. Map of extractive profiles for entrainer flow rates above and below the minimum.

a. $F > F_{min}$; b. $F < F_{min}$.

which yields for the value of the relative volatility

$$\alpha_{A,B} = \frac{y_A^*/x_A}{y_B^*/x_B} = 1 \tag{17}$$

In this case, the curve of the potential pinch points coincides with the isovolatility curve ($\alpha_{A,B} = 1$). If the flow rate of the entrainer is reduced, its concentration on the plates of the extractive section decreases. Therefore, SN moves toward vertex A until it reaches the isovolatility curve where it enters the interior of the triangle. If $F = 0$, SN coincides with the azeotropic point. These facts lead us to conclude that the minimum entrainer flow is the flow rate where (under the given vapor flow rate) the extractive section stable node is located in the intersection of the AE edge and the isovolatility curve.

The minimum entrainer flow rate can be determined based on two possibilities. If we already know a value of F where the separation is feasible ($F > F_{min}$), we can iterate F_{min} between F and 0. Since each extractive profile must arrive at SN, it is sufficient to calculate the profiles starting from a point of the still path (e.g., charge composition) under different entrainer flow rates and to choose the entrainer flow rate where SN has just moved from the AE edge, as shown in Figure 13a for $F_{min} = 0.007$ mol/s.

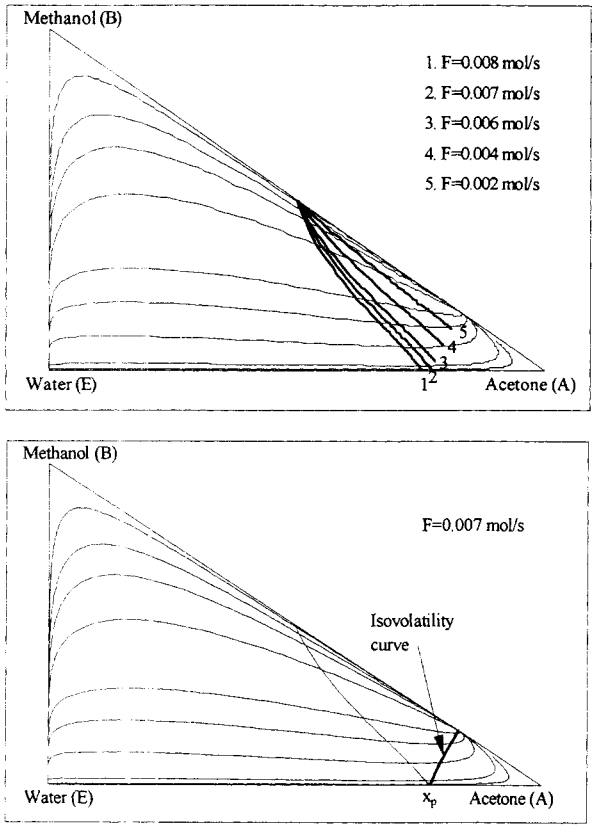

Figure 13. Methods for the determination of the minimum entrainer flow rate.

a. Determination of F_{min} by iteration; b. determination of F_{min} by the isovolatility curve.

By the second method, the following steps must be carried out. At first, the isovolatility curve, where the possible stable nodes lie, is determined (Laroche et al., 1991). For our example, the isovolatility curve is shown in Figure 13b. The extractive profiles for $F < F_{min}$ end on the isovolatility curve. In the second step, we determine the equilibrium composition of the vapor (y^*) at the point of intersection of the AE edge and the isovolatility curve (x_p). If this point is a stable node, which is the case if $F = F_{min}$, then $y = y^*$. Finally, from the value of y F_{min} is computed by using material balances:

$$F_{min} = \frac{V \cdot (x_p - y^*)}{(z - x_p)} \tag{18}$$

Being aware of the characteristics of column profiles makes possible the comparison between the continuous and the batch extractive distillation operations as for the 'unusual behavior' of these columns. Among others, Laroche et al. (1992), Wahnschafft and Westerberg (1993), and Knapp and Doherty (1994) described the unusual behavior of the continuous homoazeotropic (extractive distillation) columns, that is, an increase in the number of trays and/or reflux ratio may decrease the separation.

If the entrainer flow rate is above the minimum, every continuous extractive distillation exhibits a maximum feasible reflux. In the case of BED when F is greater than F_{min} computed for $R = \infty$, it is obvious that there is *no maximum reflux ratio*. Laroche et al. (1992, p. 1315) published a continuous example (acetone-heptane + toluene) where an increase in the number of extractive trays resulted in the decrease of the distillate purity. In the case of BED if $F > F_{min}$ (under constant heat duty) in Step 2, the extractive section stable node lies on the AE edge or it is located just outside the edge, its location depending only on the value of F. It means that if the number of extractive trays is increased, the composition of the feed tray (upper tray in the extractive section) approaches the AE edge and reaches this edge in the case of infinite number of trays. Hence, in the case of BED, if the number of trays is appropriate in the rectifying section, by increasing the number of extractive trays the maximum purity, which can be reached in Step 2, converges to a maximum value (Table 2). The specification of a minimum purity on component A means that the corresponding product composition must lie within a triangle ($\bar{x}_{D,A} > x_{D,A,spec}$). For the specified distillate purity ($x_{D,A,spec} = 0.94$), under the given F/V ratio and charge composition, there is a *minimum number of trays in the extractive section*, which is necessary for reaching the residue curve passing through the specified distillate area (triangle). However there is *no maximum number of trays* for the extractive section, since with an increase in the number of extractive trays the composition of the feed tray comes closer to the AE edge.

To study the role of the number of the rectifying trays in Step 2 [under constant heat duty and entrainer flow rate ($F > F_{min}$)] we assume that the extractive section works efficiently, that is, the number of extractive trays is sufficient and so the feed stage composition is practically located at SN. In this case, if the number of rectifying trays is too low, the entrainer, if it is too high, the less volatile component will appear at the top in a concentration too high, respectively. This can be explained by the shape of the residue curve passing through the feed stage composition assigning the possible rectifying profile. If the number of rectifying trays is increased, the top composition moves off the feed stage composition toward vertex A, and then it turns aside and moves toward the azeotropic point on the residue curve passing through the feed stage composition. By varying the number of stages the (highest) purity, which can be reached in Step 2, has a maximum (Table 3).

There is a *minimum number of rectifying trays* below which the specified distillate purity cannot be reached from the feed stage composition and there is also a *maximum number of rectifying stages* above which the rectifying profile on the residue curve leaves the triangle defined by the specified distillate purity (Figure 14) and the less volatile component contaminates the distillate to such an extent that $x_{D,A}$ decreases below its specified value.

Table 2. Influence of the Number of Extractive Trays onto the Maximum Purity Accessible in Step 2 (Rigorous Model)

N_{ES}	4	6	10	14	18	22	26
$x_{D,A,max}$	0.8918	0.9344	0.967	0.9732	0.9742	0.9743	0.9743

Table 3. Influence of the Number of Rectifying Trays onto the Maximum Purity Accessible in Step 2 (Rigorous Model)

N_{RS}	1	2	3	4	5	9	14	19	24
$x_{D,A,\max}$	0.898	0.932	0.952	0.965	0.973	0.987	0.978	0.886	0.790
$x_{D,M}$	0.001	0.001	0.001	0.002	0.003	0.007	0.021	0.114	0.210

Feasibility for Step 3

The basic difference between Steps 2 and 3 is that in the latter there is product withdrawal and the reflux ratio has a finite value. To assess the feasibility we have to find answers to the following questions. Is it possible to reach the specified distillate purity from a particular still composition at all? Can we perform an instantaneous state of column with these still and distillate compositions in Step 3? From a particular still composition the specified distillate purity can be reached if the extractive profile starting from x_S meets the rectifying profile for the specified distillate composition (x_D) under the given values of V, F and distillate flow rate (D). To answer the second question we have to investigate the still path and decide whether from an instantaneous still composition the given distillate composition can be reached or not. In this step the variation of the still composition (x_S) can be expressed by the following differential equation:

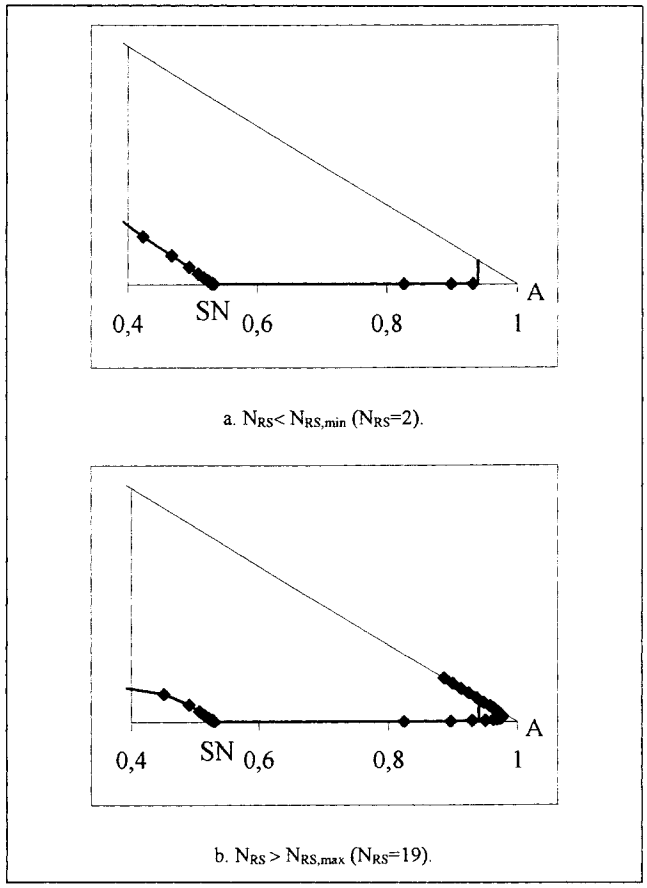

Figure 14. Rectifying profiles at the end of Step 2 when the number of rectifying trays is not appropriate ($x_{D,A,spec}$ = 0.94, rigorous model).

a. $N_{RS} < N_{RS,min}$ (N_{RS} = 2); b. $N_{RS} > N_{RS,max}$ (N_{RS} = 19).

$$\frac{d(H_S \cdot x_S)}{dt} = +F \cdot z - D \cdot x_D \tag{19}$$

where the initial condition is defined by the final state of Step 2.

The direction of the still path is a combination of the distillate withdrawal and the continuous entrainer feeding (Figure 15). The distillate withdrawal drives the still composition away from the distillate composition (vector $-D$) while the entrainer feeding pulls it toward the entrainer vertex (vector $+F$). As a resultant of the two vectors the still composition moves on a straight line starting from the still composition at the end of Step 2 [$x_S(t_2)$] until it reaches either the *BE* edge of the triangle or an extractive section stable separatrix. Figure 15 also shows the rectifying profile for the specified distillate composition.

To decide whether from a particular still composition the specified distillate composition under the given reflux ratio can be reached or not, the feasible extractive profile starting from the still composition and the feasible rectifying profile starting from the specified distillate composition must be computed by Eq. 8. If R is low, the possible rectifying profile can differ significantly from the residue curve. In this case, first the top liquid composition x_1 must be determined by dew-point calculation from x_D, and then the rectifying profile is computed from x_1 by Eq. 8. If the extractive and rectifying profiles intersect, the separation is feasible (Figure 16). Under the given conditions the separation is feasible for the majority of the possible still compositions since the majority of the extractive profiles meet the appropriate rectifying profile. However, if the still composition is near the *BE* edge the separation becomes infeasible, because these extractive profiles arrive at the *BE* edge and do not attain the appropriate rectifying profile. Since the still composition is moving toward the BE edge with time, the separation becomes infeasible at a certain point in time in Step 3.

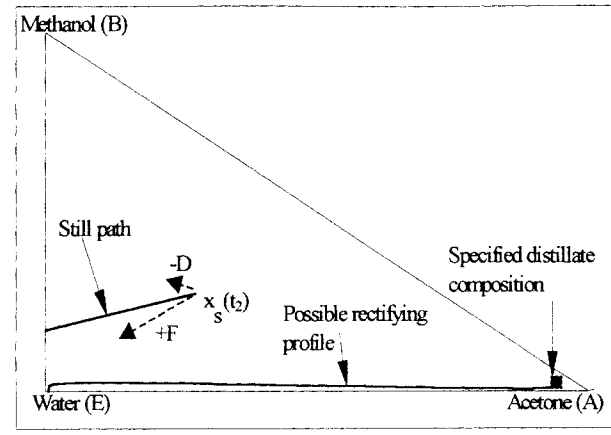

Figure 15. Still path and the rectifying profile in Step 3.

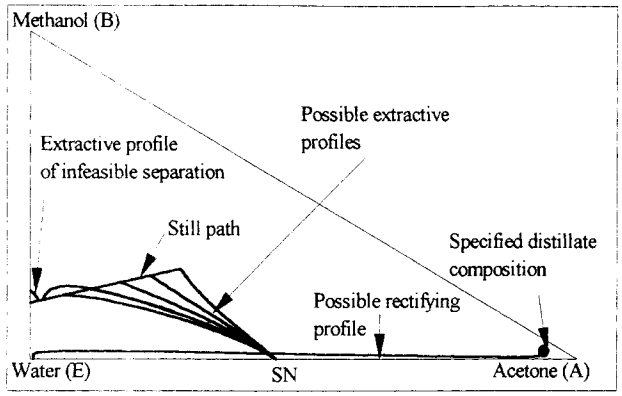

Figure 16. Possible extractive profiles in Step 3 for feasible and infeasible separations.

More information can be obtained if we draw all extractive profiles calculated by Eq. 8 under the given value of F, z, V, D, x_D and residue curves in the triangle. Figure 17 shows the feasible extractive profiles for the above experiment ($R = 4$), the residue curves and the profiles computed by rigorous simulation.

The simulated profiles show acceptable agreement with the feasible extractive profiles computed by Eq. 8 and the residue curves, respectively. The slight difference between the location of the feed stage composition and *SN* can be explained by the fact that in the course of the rigorous simulation the plate holdups and heat balances were also taken into consideration.

Figure 17 also shows that if $R < \infty$ the extractive section has a third fixed point: *UN* which originates from vertex *E* in addition to the saddle point S_2 originating from vertex *B* and the stable node *SN* coming from the azeotropic point. In our case, if the entrainer flow rate *F* and the reflux ratio *R* are varied, the location of *UN* hardly changes. On decreasing *R* (*F* remains unchanged) S_2 moves toward the *AE* edge and *SN* comes nearer to vertex *E*.

When the map of the feasible profiles is computed, F, z, V, D, x_D must be kept constant. If we want to draw conclusions for the whole step, we have to control the constancy

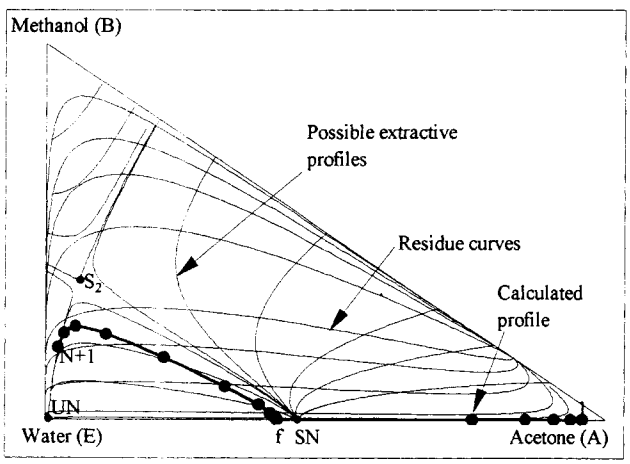

Figure 17. Simulated column profile in the map of extractive and rectifying profiles.

$t = 195$ min; $\Delta t_2 = 78$ min.

of these parameters. The composition of the entrainer is always constant. If *R* and *F* are kept constant under constant heat duty (Q_{N+1}), *V* and *D* are approximately constant, too. (The assumption of constant molar overflow provides a proper approximation in the majority of the cases.) The constancy of x_D is not evident. Figure 6 shows that during almost the whole production step (in spite of the constancy of *R*) the distillate composition was practically constant, because even though x_S varies with time if the number of extractive stages is sufficiently high, all extractive profiles approach the stable node on the *AE* edge (Figure 17). Therefore, the rectifying profile starts practically from the stable node in any case, so x_D remains nearly constant for the most part of Step 3.

On the basis of these facts we can draw conclusions for the characteristics of Step 3 using the map of the possible extractive profiles shown in Figure 18. In the case of a finite reflux ratio the saddle-point S_2 divides the triangle into four regions with its four separatrices (for continuous extractive distillation, see Knapp and Doherty, 1994). From Regions I and II the possible extractive profiles arrive at the *AE* edge. If the still composition lies in these regions, the BED separation is feasible. However, from Regions III and IV, the possible extractive profiles do not arrive at the *AE* edge, but they reach the BE edge. If the still composition lies in these regions, the BED separation is infeasible. Hence, for the given values of *F*, *z*, *V*, *D* and x_D we can define an infeasible region consisting of Regions III and IV. When the still composition reaches the boundary of the infeasible region (stable separatrix) that the still path cannot cross, the specified product composition cannot be maintained any longer and the distillate composition will move toward vertex *B*.

From a mixture with fixed acetone content (e.g., $x_A = 0.1$) the specified distillate product with the given entrainer flow rate and composition cannot be obtained by extractive distillation if the methanol concentration is high (to the detriment of water content) whereas it can be obtained, if the methanol concentration is low (Figure 18). This conclusion agrees with our experimental and simulation results. Figure 18 also shows that the infeasible region becomes narrower toward vertex *E*. The smaller the distance between the still composition and the *BE* edge at the end of Step 3, the higher the recovery of *A* (assuming the same conditions as for Step 2). Therefore, in the case of BED the favorable still paths move toward vertex *E*.

The middle vessel column is basically a batch rectifier on the top of a batch stripper with a common still pot (Safrit et al., 1997). If a middle vessel column is operated under the same conditions in the rectifying and extractive sections, the infeasible region will be the same as that for a batch rectifier. It means that if the still path is steered toward vertex *B*, recovery of *A* will be smaller than that by steering the still path toward vertex *E*. Since in the case of finite reflux ratios vertex *B* is in the infeasible region (saddle point S_2 originating from *B*) a recovery of 100% cannot be even theoretically obtained by a middle vessel column. Therefore, we find the statement by Safrit et al. (1995, p. 3262) misleading that in the case of BED in a middle vessel column a recovery of 100% of component *A* is theoretically possible in a three-component mixture, when the still path is steered toward the intermediate component. Figure 19 shows the difference between the 'infeasible' regions, which could be obtained

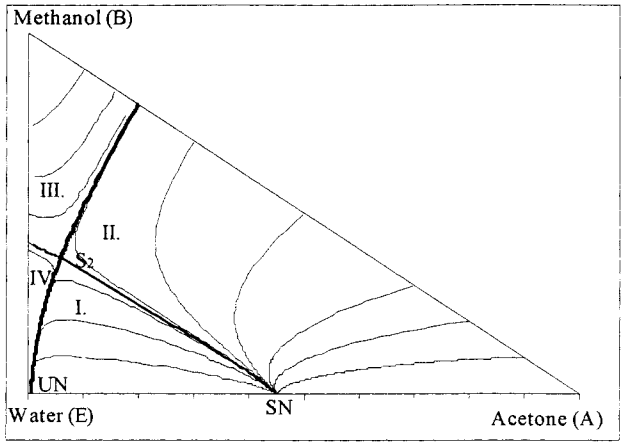

Figure 18. Map of possible extractive profiles, feasible and infeasible regions.

by the method of Safrit et al. (1995) and the real infeasible regions for a given set of parameters. For a still composition in each of the regions IR, FR_1 and FR_2, by the simulation of an instantaneous state of the column ($f = 6$, $R = 4$, $V = 0.048$ mol/s, $F = 0.0278$ mol/s, $z = [0.0, 0.0, 1.0]$ and $x_{S,IR} = [0.1, 0.8, 0.1]$, $x_{S,FR1} = [0.035, 0.200, 0.765]$, $x_{S,FR2} = [0.9, 0.05, 0.05]$, respectively) from FR_1 and FR_2 with a limited number of stages ($N = 18$) we attained acetone purity ($x_{D,A}$) significantly higher than 0.94. [The above calculation was made with the continuous rigorous module using simultaneous correction method of the simulator CHEMCAD III (1997).] However, from IR only the azeotropic composition was reached even with 100 stages since the extractive profile ran to a fixed point [0.026, 0.338, 0.636] far from the AE edge. Below the point S_2 the real infeasible region is much smaller because the region FR_1 is in fact feasible. However, above S_2 the real infeasible region is much greater since the region IR is infeasible. The region FR_2 near vertex A qualified infeasible by the method of Safrit et al. (1995) is feasible.

The recoveries accessible by BED in a batch rectifier and in a middle vessel column can be compared by mass balance calculations. Figure 15 shows the still path for the batch rectifier. The maximum recovery can be estimated based on the point where the still path and the boundary intersect be-

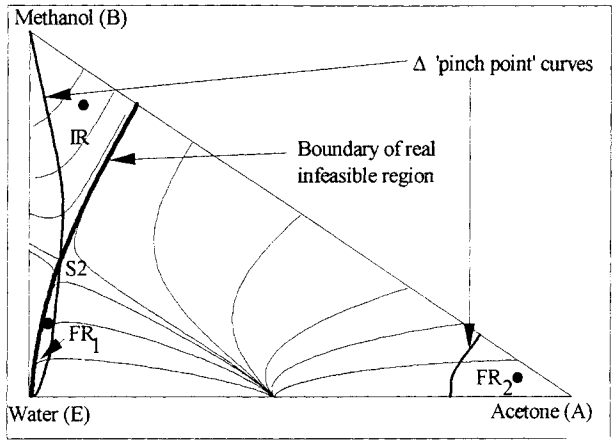

Figure 19. Comparison of the boundary and Δ 'pinch point' curves.

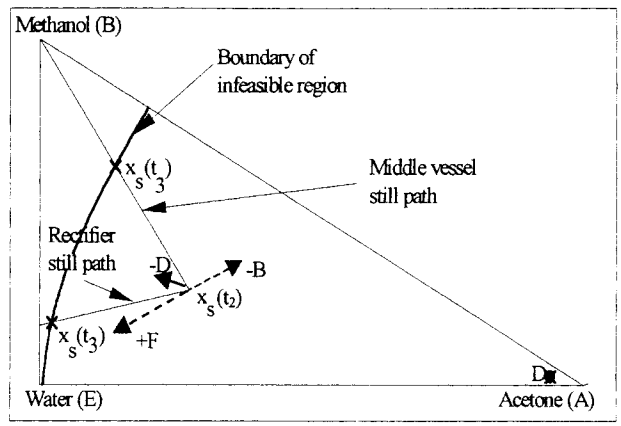

Figure 20. Comparison of the still path of a batch rectifier and that of a middle vessel column.

tween the infeasible and feasible regions (Figure 20). From the still composition at the beginning and at the end of the production step, the recovery of A can be calculated from mass balances written for this step. For the middle vessel column by the suggestion of Safrit et al. (1997), a still path moving toward vertex B is selected from the same starting point $x_S(t_2)$.

This still path determines the flow rate of the bottom product of a given composition (pure water). Then, the intersection of the still path and the boundary gives the final still composition in the production step. In our case, the maximum recovery was 88% for the batch rectifier and 78% for the middle vessel column.

In the case of infinite reflux ratio (Step 2), the whole triangle is feasible since the boundary is the BE edge itself. On reducing the reflux ratio the area of the feasible region decreases (Figure 21). The shape of the boundaries under different reflux ratios indicates that the recovery of the middle vessel column is lower for all reflux ratios than that of the batch rectifier. However, the increase of the reflux ratio decreases the difference between the two recoveries.

There is a *minimum reflux ratio* under which each point of the still path in Step 2 is located in the infeasible region. In our case, $R = 1.5$ is above, $R = 0.6$ is below the minimum reflux ratio for the extractive section. At the minimum value of the reflux ratio, the still path is a tangent to the boundary.

The *minimum entrainer flow rate* for Step 3 is lower than its value for Step 2 if under the given reflux ratio the separation is feasible at all, since the reduction of the reflux ratio increases the concentration of the entrainer on the stages and in the case of our mixture $\alpha_{A,B}$ rises with increasing x_E in a monotone way. The method of the determination of $F_{\min}$ is similar to that applied in Step 2, but in Step 3 the curve of the potential pinch points does not coincide with the isovolatility curve. Though $F_{\min}$ can be determined for finite values of R the application of an entrainer flow rate lower than $F_{\min}$ ($R = \infty$) is not recommended in engineering practice because it is not economical (it results in a very low recovery). It is still worth mentioning—though it has no importance in engineering practice—that for $F < F_{\min}(R = \infty)$, if the separation is feasible for this entrainer flow rate, there is also a maximum reflux ratio (Figure 22).

At reflux ratios lower than the maximum the stable node is located on the AE edge or outside the triangle and there is a

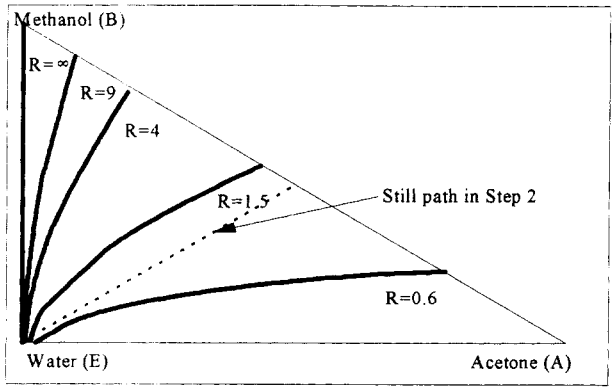

Figure 21. Influence of the reflux ratio onto the size of the infeasible region.

reflux ratio (in our case $R \sim 31$) above which the stable node gets into the interior of the triangle.

Feasibility of Step 4

The production of the more volatile component is finished when, under constant reflux ratio and entrainer flow rate (basic operational policy), the prescribed distillate purity cannot be maintained any longer because the still composition had reached the boundary of the feasible region for the extractive section which cannot be crossed. The entrainer feeding is then stopped. In Step 4 the less volatile component is separated from the entrainer (in the simplest case under constant reflux ratio, obviously without entrainer feeding). The extractive section does not exist any more and the whole column operates as a rectifying section. Therefore, the feasibility method of Bernot et al. (1991) can be applied for the determination of the possible cuts (e.g., taking an intermediate cut) depending on the still composition at the end of Step 3. In the case of large reflux ratio, the liquid composition profiles in the column follow the simple distillation residue curves, so the distillate and the still compositions are on the same residue curve. In the case of low reflux ratios, the possible profiles can differ significantly from the residue curves and therefore must be computed in the way described earlier.

The acetone (A) remaining in the still after Step 3 can be withdrawn in the intermediate cut and recycled. While the

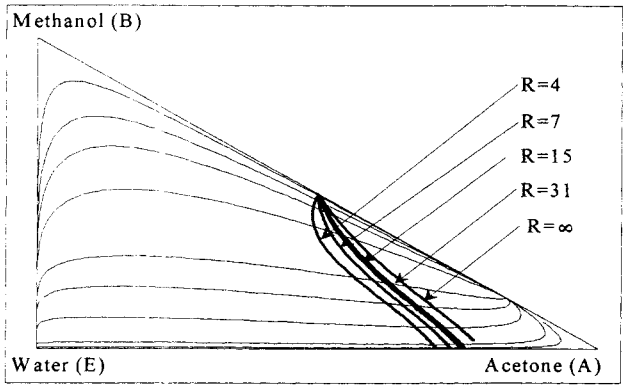

Figure 22. Maximum reflux ratio for Step 3 ($F = 0.006$ mol/s).

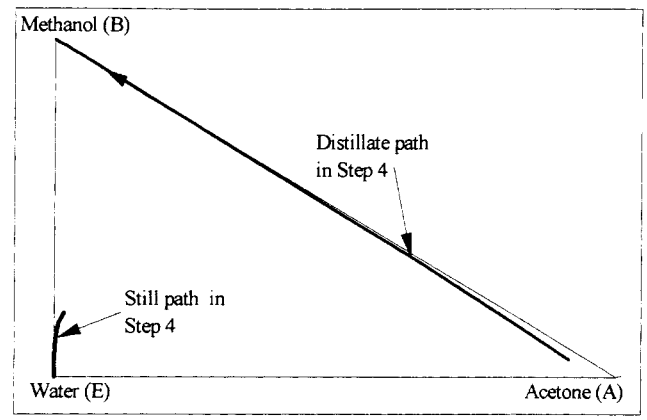

Figure 23. Evolution of the distillate and still compositions in Step 4.

intermediate cut is being taken, the distillate composition moves from the neighborhood of vertex A toward vertex B. When the whole quantity of A had already been withdrawn a simple binary B/E separation is carried out. The evolution of the distillate and still compositions in Step 4 are shown in Figure 23.

Conclusion

A feasibility method was developed for performing the batch extractive distillation (BED) in a batch rectifier and demonstrated by a pilot-plant experiment (with the mixture acetone-methanol+water). For the same experiment the feasibility method of Safrit et al. (1995) did not yield proper results. However, the results obtained by our method agreed with the experiments.

For the calculation of the composition profiles of the extractive and rectifying sections of the column a simple dynamic model was developed. Feasibility means that for a given composition mixture a specified distillate composition can be reached by BED with the entrainer of given composition. The separation is considered feasible if such an instantaneous state of the column exists, which provides the required quality distillate starting from the charge of the given composition.

Based on the map of possible extractive profiles and residue curves for Step 2, we can determine the feasibility, the sequence of the components in the product, and the minimum entrainer flow rate. The necessary and sufficient condition of the feasibility is to have at least one extractive section profile linking the still path with the possible rectifying profile. The sequence of the components depends on the location of the extractive section stable node. If it lies on the AE edge (or behind it) component A, if it is on the BE edge (or behind it) component B can be obtained as top product in the first production step (Step 3). If the separation is feasible with a particular entrainer flow rate there must be a minimum flow rate (F_{min}), since the separation is infeasible for $F = 0$. The determination of F_{min} is based on the fact that if the value of the entrainer flow rate is decreased below its minimum value the extractive section stable node gets into the interior of the triangle.

We concluded that in the case of sufficiently high entrainer flow rates there is no maximum reflux ratio. For a minimum

distillate purity prescribed ($x_{D,A,\text{spec}}$) there is a minimum number of stages of the extractive section, but there is no maximum. For this purity, both a minimum and a maximum number of rectifying stages can be computed.

In Step 3 under the given values of parameters for the extractive section, an infeasible region can be determined. If the still composition is located within this region, an appropriate separation A/B cannot be obtained. The batch rectifier was compared with the middle vessel column, and we arrived at the conclusion that by the middle vessel column a smaller recovery of A can be obtained under the same conditions (in our case, the difference was about 10%).

Notation

f = feed plate number
h = plate number
H = holdup, mol
L = liquid flow rate, mol/s
P = pressure, bar
Q = heat duty, kW
S_2 = saddle point of the extractive section
SN = stable node of the extractive section
t = time, min
UN = unstable node of the extractive section
V = vapor flow rate, mol/s
x = liquid mole fraction
y = vapor mole fraction
z = entrainer mole fraction
α = relative volatility
Δ = difference, delta point
η = recovery

Subscripts

A = more volatile component, acetone
az = azeotrope
B = less volatile component
C = condenser
D = distillate
E = entrainer
ES = extractive section
j = plate
M = methanol
max = maximum value
min = minimum value
RS = rectifying section
S = still pot
spec = specified value
W = water

Superscripts:

vol = volumetric
$*$ = equilibrium

Acknowledgments

The authors are grateful to Prof. Sandor Kemeny (TUB) and Prof. Michel Otterbein for their valuable help. This research was financially supported by the Hungarian National Research Foundation ("OTKA") under grant T 016853.

Literature Cited

Ahmad, B. S., and P. I. Barton, "Homogeneous Multicomponent Azeotropic Batch Distillation," *AIChE J.*, **42**, 3419 (1996).

Berg, L, and An-I Yeh, "The Unusual Behavior of Extractive Distillation (Reversing the Volatility of Acetone-Isopropyl Ether System," *AIChE J.*, **31**, 504 (1985).

Bernot, Ch., M. Doherty, and M. F. Malone, "Patterns of Composition Change in Multicomponent Batch Distillation," *Chem. Eng. Sci.*, **45**, 1207 (1990).

Bernot, Ch., M. Doherty, and M. F. Malone, "Feasibility and Separation Sequencing in Multicomponent Batch Distillation," *Chem. Eng. Sci.*, **46**, 1311(1991).

Chemstations, *CHEMCAD III, Process Flowsheet Simulator*, Chemstations Inc., Houston (1997).

DiStefano, G. P., "Mathematical Modeling and Numerical Integration of Multicomponent Batch Distillation Equations," *AIChE J.*, **14**, 190 (1968).

Doherty, M. F., and G. A. Caldarola, "Design and Synthesis of Homogeneous Azeotropic Distillations: 3. The Sequencing of Columns for Azeotropic and Extractive Distillation," *Ind. Eng. Chem. Fundam.*, **24**, 474 (1985).

Doherty, M. F., and J. D. Perkins, "On the Dynamics of Distillation Process: III. The Topology Structure of Ternary Residue Curve Maps," *Chem. Eng. Sci.*, **34**, 1401 (1979).

Fidkowski, Z. T., M. F. Malone, and M. F. Doherty, "Nonideal Multicomponent Distillation: Use of Bifurcation Theory for Design," *AIChE J.*, **37**, 1761 (1991).

Fidkowski, Z. T., M. F. Doherty, and M. F. Malone, "Feasibility of Separations for Distillation of Nonideal Ternary Mixtures," *AIChE J.*, **39**, 1303 (1993).

Gmehling, J., U. Onken, and W. Arlt, *VLE Data Collection*, DECHEMA, Frankfurt (1977).

Griswold, J., and C.B. Buford, *Ind. Eng. Chem.*, **41**, 2347 (1949).

Knapp, J. P., and M. F. Doherty, "Minimum Entrainer Flows for Extractive Distillation: a Bifurcation Theoretic Approach," *AIChE J.*, **40**, 243 (1994).

Kohler, J., H. Haverkamp, and N. Schadler, "Discontinuous Rectification of Azeotropic Mixtures with Use of Auxiliary Substances," *Chem. Ing. Tech.*, **67**, S967 (1995).

Laroche, L., N. Bekiaris, H. W. Andersen, and M. Morari, "Homogeneous Azeotropic Distillation: Comparing Entrainers," *Can. J. of Chem. Eng.*, **69**, 1302 (1991).

Laroche, L., N. Bekiaris, H. W. Andersen, and M. Morari, "The Curious Behavior of Homogeneous Azeotropic Distillation: Implication for Entrainer Selection," *AIChE J.*, **38**, 1309 (1992).

Lang, P., H. Yatim, P. Moszkowicz, and M. Otterbein, "Batch Extractive Distillation Under Constant Reflux Ratio," *Comput. Chem. Eng.*, **18**, 1057 (1994).

Lang, P., Z. Lelkes, P. Moszkowicz, M. Otterbein, and H. Yatim, "Different Operational Policies for the Batch Extractive Distillation," *Comput. Chem. Eng.*, **19**, S645 (1995).

Lelkes, Z., P. Lang, P. Moszkovicz, B. Benadda, and M. Otterbein, "Batch Extractive Distillation: the Process and the Operational Policies," *Chem. Eng. Sci.*, accepted (1997).

Matsuyama, H., and H. Nishimura, "Topological and Thermodynamic Classification of Ternary Vapor-Liquid Equilibria," *J. Chem. Eng. Japan*, **10**, 181 (1977).

Safrit, B. T., A. W. Westerberg, U. Diwekar, O. M. Wahnschafft, "Extending Continuous Conventional and Extractive Distillation Feasibility Insights to Batch Distillation," *Ind. Eng. Chem. Res.*, **34**, 3257 (1995).

Safrit, B. T., and A. W. Westerberg, "Improved Operational Policies for Batch Extractive Distillation," *Ind. Eng. Chem. Res.*, **36**, 436 (1997).

Van Dongen, D. B., and M. F. Doherty, "Design and Synthesis of Homogeneous Azeotropic Distillations: 1. Problem Formulation for a Single Column," *Ind. Eng. Chem. Fundam.*, **24**, 454 (1985).

Wahnschafft, O. M., and A. W. Westerberg, "The Product Composition Regions of Azeotropic Distillation Columns: 2. Separability in Two-Feed Columns and Entrainer Selection," *Ind. Eng. Chem. Res.*, **32**, 1108 (1993).

Wahnschafft, O. M., J. W. Koehler, E. Blass, and A. W. Westerberg, "The Product Composition Regions of Single Feed Azeotropic Distillation Columns," *Ind. Eng. Chem. Res.*, **31**, 2345 (1992).

Yatim, H., P. Moszkowicz, M. Otterbein, and P. Lang, "Dynamic Simulation of a Batch Extractive Distillation Process," *Comput. Chem. Eng.*, **17**, S57 (1993).

Yatim, H., "Etude Théorique et Expérimentale du Procédé de Distillation Extractive Discontinue," PhD Thesis, INSA de Lyon (1993).

Manuscript received Aug. 4, 1997, and revision received Dec. 23, 1997.